

ENHANCED DELINEATION OF GLACIAL CLASTIC RESERVOIRS BY THE APPLICATION OF PETRO-ELASTIC WELL CORRELATION AND SEISMIC INVERSION: CASE STUDY

Abubaker Alansari^{1*}, Ahmed Mohamed Ahmed Salim¹, Hammad Tariq Janjuhah¹, Nuri Mohamed Fello²

¹ Department of Geosciences, University Technology PETRONAS, 32610, Perak, Malaysia

² National Oil Corporation (NOC), Tripoli, Libya

Received January 23, 2018; Accepted April 23, 2018

Abstract

The Murzuq Basin is an intracratonic basin located in the South and Southwest (SW) Libya. Glacial Ordovician sandstones are the primary reservoir. However, identifying the top of the upper Ordovician reservoir and the interpretation of intra-Ordovician sequence directly from seismic using conventional methods are well-known challenges in the exploration and production of Murzuq basin. Even with the advent of 3D seismic and dense well database. Therefore, a detailed seismic and well data analysis of the study area was carried out. Sand-shale elastic baseline cut-offs and Vp and Vs cross-over were incorporated into the petro-elastic wireline interpretation. Also, post-stack seismic inversion was applied to generate elastic attributes (acoustic impedance and modelled VpVs). Vp and Vs cross-over successfully outlined the sand cycles when the Vp is located on the right side of the track, whereas the appearance of Vp on the left side indicates the presence of shale units. Seismic inversion provided a better lateral continuity and vertical top and inter reservoir events separation, which has improved their traceability. The VpVs attribute illuminated the reservoir area by the low percentage ratios of 1.6 and 1.8, which is the expected range for sand bodies with emphasis to their upper, mid and lower contacts. Hence, elastic properties derived from both wells and seismic enhanced the delineation of the top of the Upper Ordovician unconformity unit of Mamuniyat Formation (top reservoir) and enabled clear distinction between a non-reservoir unit of upper Ordovician formation (Bir-Tlaksin) and the primary reservoir.

Keywords: Upper Ordovician reservoir; Petroleum system; Post stack seismic inversion; Petro-elastic; Murzuq basin.

1. Introduction

The Murzuq Basin is one of a range of North African intracratonic basins. It is located in south-west Libya, covering some 35,000 km², which is filled with sediments that range in age from the Precambrian to Quaternary. The Gergaf Arch borders the basin to the north, the Thimboka Arch to the west and the Tibisti Arch to the east (Figure 1). Former studies have demonstrated that the structural evolution of the basin was a result of several distinct major tectonic phases that affected the whole North Africa [1]. These phases include the Pan-African orogeny in the Precambrian; Cambrian extension; Cambrian to Carboniferous alternating extension and compression; late Carboniferous (Hercynian) uplift; late Triassic-Early Jurassic and early Cretaceous rifting, mid-Cretaceous (Austrian); late Cretaceous-Tertiary (Alpine) compression; Neogene-Recent uplift, and volcanic activity (Figure. 2) [1-4].

The Murzuq Basin is considered to be one of the producing areas in Libya with recoverable oil volume of 2300 MMbl [4-6]. As a result, the basin has been prioritised for extensive exploration activities, especially after the discovery of the giant Elephant oil field by British Operator Lasmo in 1998 [7]. The increase in oil prices in the mid-1990s to early 2000s (albeit with fluctuations) allowed oil companies to invest in exploration, even in isolated areas with costly exploration fees. Accordingly, some multi-international oil companies increased their explora-

tory operation within the basin and succeeded in adding several oil discoveries to the near oil field exploration campaigns in North-West Murzuq basin. However, all exploration efforts made in the South- SW part of the basin has been suspended without announcing any economic findings.

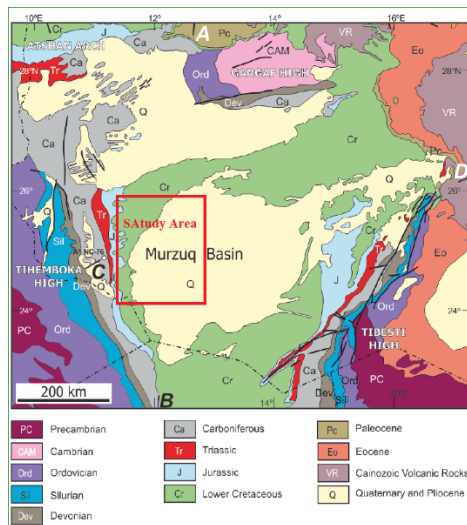


Fig. 1. The boundary of Murzuq Basin and study area location edited from (Shalbak [19])

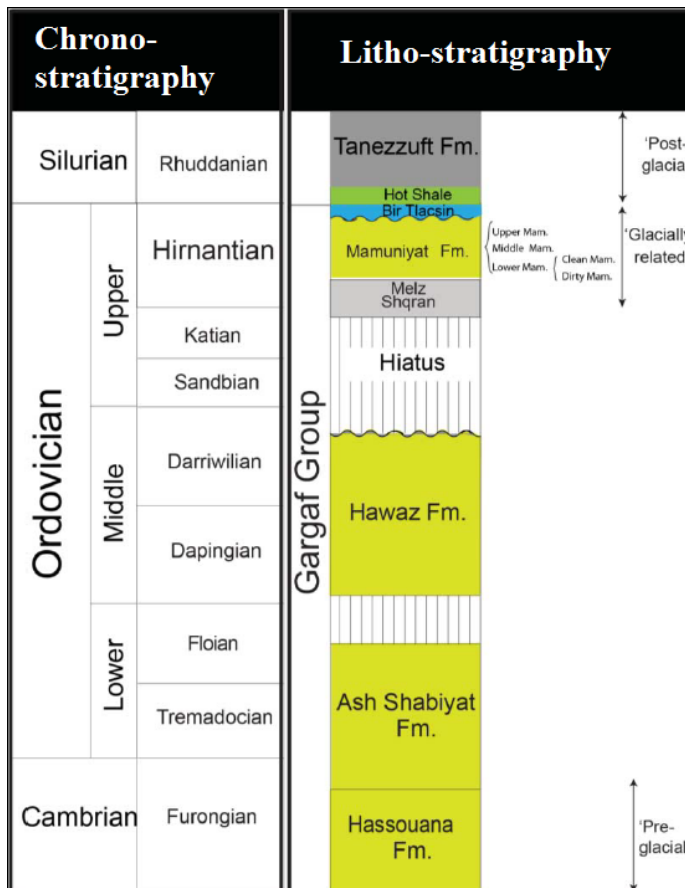


Fig. 2. Stratigraphic column of Murzuq basin (McDougall [24])

The absence of any high-quality dataset and the interpretation of existent ones in the south-SW Murzuq basin has severely affected the outcome of the exploration activities on this side of the basin. Meanwhile, only 2D seismic data were acquired in the latest exploration activities. Furthermore, identifying the tops and bottom of upper Ordovician reservoir unit as well as the interpretation of intra-Ordovician sequence are well-known pitfalls in the exploration and production of Murzuq basin, even with the advent of 3D seismic and dense well database [8]. It has been a frequent practice to use the lower contact of Silurian hot-shale as a top reservoir in all Murzuq basin. Due to it is strong continues reflection resulted from strong impedance contrast between the Silurian shale and underlying Ordo-vician sand. Therefore, attention has been drawn in the latest years to the incorporation of pre and post-stack seismic inversions into latest studies. Especially in the Northern part of the basin, such as the con temporary study by [9],

which used coloured inversion to improve the detection of this reservoir. However, to the best of our knowledge, pre and post-stack seismic inversions are yet to be applied to the South-SW part of the basin.

Therefore, this paper is an attempt to enhance the delineation of the upper Ordovician reservoir by integration of petro-elastic interpretation methods to the available database at South-SW part of the Murzuq basin.

The results will provide the basis to identify reservoir characteristics from seismic and wells. Also, overcoming the traditional practice of picking the bottom of lower Silurian (strong negative impedance) source rock as the top reservoir contact. Achieving the objectives will ensure that the factors controlling the delineation of the upper Ordovician reservoir in the Southwestern part of the Murzuq Basin are rationally examined through the interpretation of inverted well calibrated post-stack seismic data.

2. Petroleum system elements

There are three proven oil reservoirs in the Murzuq Basin (SW Murzuq), namely: Ordovician sandstones of Hawaz; Ordovician sandstones of Mamuniyat, and Devonian sandstones of the Awaynat Wanin Formation [10]. The Silurian Tanezzuft Formation is the primary source rock for the Basin and also provides the regional seal for the Ordovician reservoirs (Figure. 2). For this paper, the only upper Ordovician reservoir (Mamuniyat Fm.) of Lower Palaeozoic plays (Ordovician sandstones of Hawaz and Mamuniyat) will be covered.

2.1. Reservoirs

The reservoir varies across the Murzuq Basin between Mamuniyat and Hawaz, while a combination of both characterises some areas. The Mamuniyat Formation consists of sandstones that are medium to coarse-grained, and moderately to poorly sorted. The sandstones are clean, with porosity varying from 7% up to 20% with an average of 11%, while their permeability can reach 1600 mD with an average of 300 mD. The reservoir properties of the Hawaz formation are moderated by the amount of fluvio-tidal channels present in the primary reservoir zones. The average porosity of the Hawaz reservoir is approximately 13% with permeability values ranging between 1-20 mD in the Lower Shoreface facies and up to 50-700 mD in the channel facies [11].

2.1.1. Hawaz Formation

Some studies have characterised the depositional environment of Hawaz Formation as a gently dipping shelf covered by epicontinental seas with a broad coastal plain area that is fragmented by channels [12-13]. The models of the Hawaz Formation consist of a sequence of stacked sedimentary packages. That belongs to the shelf (burrowed) and lower shoreface facies association in the bottom part, followed by fining upwards fluvio-tidal channel sandstones in the middle part, which are overlain by burrowed shelf and lower shoreface sediments in the uppermost part. These sedimentary rocks were intensely eroded and carved by ice streams afterwards (late Ordovician glaciation) to form a unique terrain of cliffs and incised valleys [14].

2.1.2. Mamuniyat Formation

The Mamuniyat Formation depositional environment is interpreted as a relatively deep marine, to fluvial sedimentary sequence [15-16]. Massive volumes of outwash sands and gravel were deposited over a glacial-fluvial outwash plain due to the melting of glacial overburden. Braided deltas were subsequently developed where the outwash streams come in contact with the coastline [17]. In some areas, these deltas prograded across a thin shelf until their transported sediment was redeposited in the edges and borders of turbiditic fans. The coarse glacial-fluvial sands were then reworked in a shallow marine environment to generate near-shore bar features away, in sheltered areas between the braided deltas [17]. The Top Mamuniyat Formation consists of a lower unit of coarse-grained braided channel sandstones

and deposits covered by the very coarse-grained unit. While the Middle Mamuniyat is a heterogeneous mix of fine-grained delta front to delta plain sediments in the lower part, which are abruptly covered by coarser grained delta plain/distributary channel sediments [18]. The Lower Mamuniyat is also variable and comprises primarily fluvial distributary channel and shallow marine sandstones [10,12,19].

3. Dataset and methodology

The study area is covered by a dense 2D seismic grid that was acquired in different stages. Moreover, some exploration and water wells are drilled. However, only three wells (Brine Sands) will be used for this study.

3.1. Well data

The wells drilled in the area were correlated to obtain them. All the wells have relevant wireline logs that include Gamma-ray (GR), Resistivity, Sonic, Neutron and Density logs from which the vertical distribution of the petroleum system members within this region and accurate synthetic seismograms were derived (Figure 3).

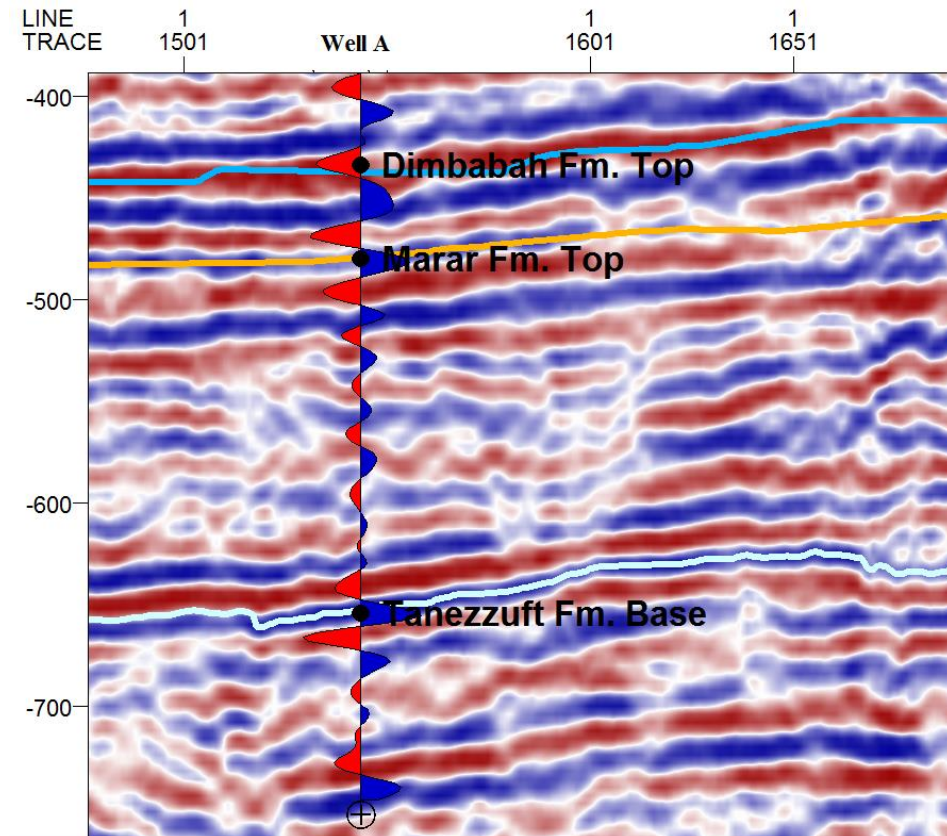


Fig. 3. Seismic well tie used for conventional seismic interpretation

3.1.1. Petrophysical interpretation of wireline logs

$$V_{sh} = \frac{GR_{log} - GR_{min}}{GR_{max} - GR_{min}} \quad (1)$$

For porosity determination, a combination method of neutron porosity, density and sonic logs will be applied to obtain more favourable total porosity (ϕ_{total}) (Asquith and Gibson 1982).

$$\phi_N = \text{Neutron Porosity from the logs} \quad (2)$$

$$\phi_D = \frac{\rho_{ma} - \rho_{log}}{\rho_{ma} - \rho_{fl}} \quad (3)$$

where: ϕ_D = density porosity; ρ_{ma} = matrix density; ρ_{log} = bulk density from log and ρ_{fl} = Fluid density.

$$\phi_S = \frac{\Delta t_{log} - \Delta t_{ma}}{\Delta t_{fl} - \Delta t_{ma}} \quad (4)$$

where: ϕ_S = sonic derived porosity; Δt_{ma} = matrix transit time; Δt_{log} = sonic transit time from log and Δt_{fl} = fluid transit time.

After that total porosity will be obtained by averaging three determined porosity types above (density, neutron and sonic)

$$\phi_{total} = \frac{\phi_S + \phi_D + \phi_N}{3} \quad (5)$$

3.1.2. Estimation of elastic properties of reservoir rocks

For the three wells available for this study, compressional sonic log is available, but the shear wave sonic exist in only one well

3.2.1. Share wave estimation (Vp) and Vp/Vs ratio

Several methods will be used for Vs estimation; these methods included Castagna "mudrock line", Greenberg-Castagna, and correlation regressions. After that, the above methods will be compared, and one of them will be selected based on its accuracy when compared to the measured Vs from well A.

3.2.2. Gassman fluid substitution

The wells used here represents brine sands which caused a lower impedance contrast between shale and sand unit. Therefore, Gassmann fluid substitution is applied (100% brine and 70 % oil & gas) to improve the P-impedance contrast if gas case logs used as input for post-stack seismic inversion. Below here is workflow of the substitution

$$K_{sat} = K_{dry} + \frac{\left(1 - \frac{K_{dry}}{K_{sat}}\right)^2}{\frac{\phi}{K_f} + \frac{1-\phi}{K_{ma}} - \frac{K_{dry}}{K_{ma}^2}} \quad (6)$$

$$\mu_{sat} = \mu_{dry} \quad (7)$$

where K_{dry} , K_f And K_{ma} are the bulk moduli of the dry rock, trapped fluids and rock matrix (GPa) respectively; and ϕ is the fractional porosity of the rock .Shear moduli of the dry and saturated rock (GPa) are denoted by μ_{dry} and μ_{sat} , respectively. It is worth stating that corrected log derived density values were used as an input for ρ_{sat} and ρ_{ma} (density of saturated and matrix rock). These density values were derived from the equation below.

$$\rho_{fl} = S_w \rho_w + (1 - S_w) \rho_{hc} \quad (8)$$

where, S_w is water saturation, ρ_w = density of formation water and ρ_{hc} = density of hydrocarbon. The mass balance equation will be used for calculating the bulk density of the mixed fluid rock;

$$\rho_b = \rho_g + (1 - \phi) \rho_{fl} \quad (9)$$

ρ_b = bulk density; ρ_g = formation's grain density; ϕ = total porosity and ρ_{fl} is density of the fluid occupying the pores.

Then, fluid modulus will be estimated by using Wood's equation;

$$K_{fl} = \left(\frac{S_w}{K_w} + \frac{(1-S_w)}{K_{hc}}\right)^{-1} \quad (10)$$

where, K_{fl} is Fluid modulus, K_w represents bulk modulus of brine and K_{hc} denotes hydrocarbon bulk modulus.

Elastic properties of a medium (the compressional and shear wave velocity of a rock), V_p and V_s , can be estimated for any saturation by using the equations below;

$$Vp = \sqrt{\frac{K_{sat} + 4\mu_{sat}/3}{\rho_{sat}}} \tag{11}$$

$$Vs = \sqrt{\frac{\mu_{sat}}{\rho_{sat}}} \tag{12}$$

where K_{sat} and μ_{sat} are the bulk and shear moduli of saturated rock (GPa), respectively, while the ρ_{sat} is the bulk density of saturated rock (g/cm^3). The bulk and shear moduli of saturated

3.2. Seismic data

The conventional seismic data interpretation was constrained to three wells (A, B and C). Five Horizons were identified (Top Zarzartine, Top Tigouentourine, Base Tanezzuft, Top Mamuniyat and Basement) and tied to the wells. However, for this study, three horizons (Basement, Ordovician Base Tanezzuft and Permian Top Tigouentourin) were prioritised and wholly interpreted. Ordovician Base Tanezzuft shale is the critical horizon that can be traced easily within the area since it directly overlies the critical Ordovician sandstone reservoirs, hence it has frequently been used for the mapping. Synthetic Seismogram was generated using check-shots data, corrected sonic and density, which were then tied to the seismic for calibration and referenced to interpreted 2D seismic lines. After that, the study area was mapped based on the seismic interpretation. Finally, two seismic lines that cross through well A&C were selected as a candidate for post-stack seismic inversion analysis

3.3. Post Stack Seismic Inversion

In this paper, two post-stack 2D seismic lines (X&Y) (Figures 4. 5), which cross through two wells (C and A), were inverted using model-based inversion where the acoustic impedance was calculated at each well location before wavelet estimation and seismic well tie (Figure. 6). A reasonable match between seismic and synthetic data was achieved with only 3 ms shift was applied (Figure. 6).

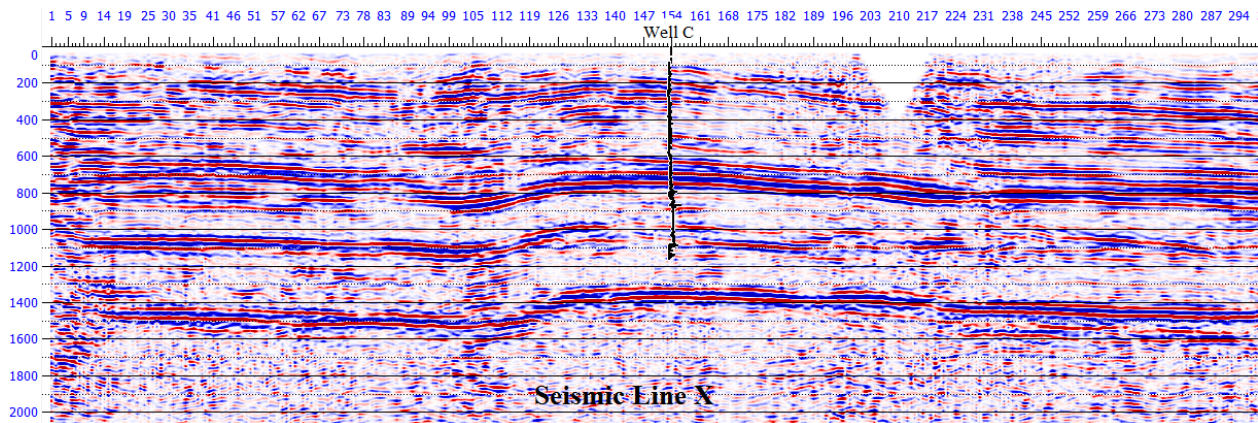


Fig. 4. 2D seismic section X

3.3.1. Vp/Vs Computation

For Vp/Vs modelling inverted acoustic impedance and original seismic lines will be used as an input for multi-attribute analysis and neural network training for both seismic lines. Then the multi-seismic attributes and neural network will be used to generate the relationship which then calibrated with the estimated Vp/Vs from the wells before applying it to the seismic lines.

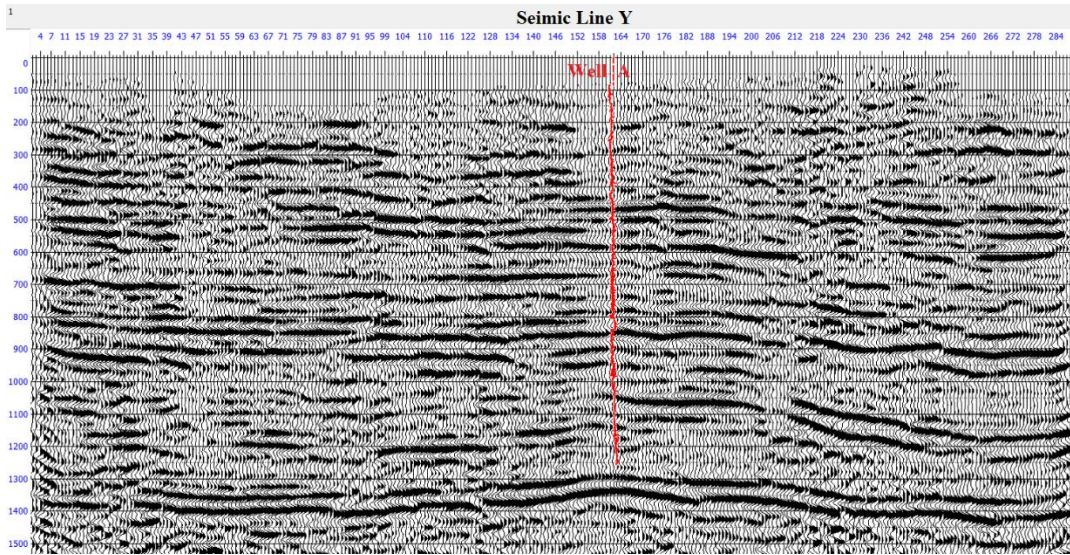


Fig. 5. 2D seismic section Y

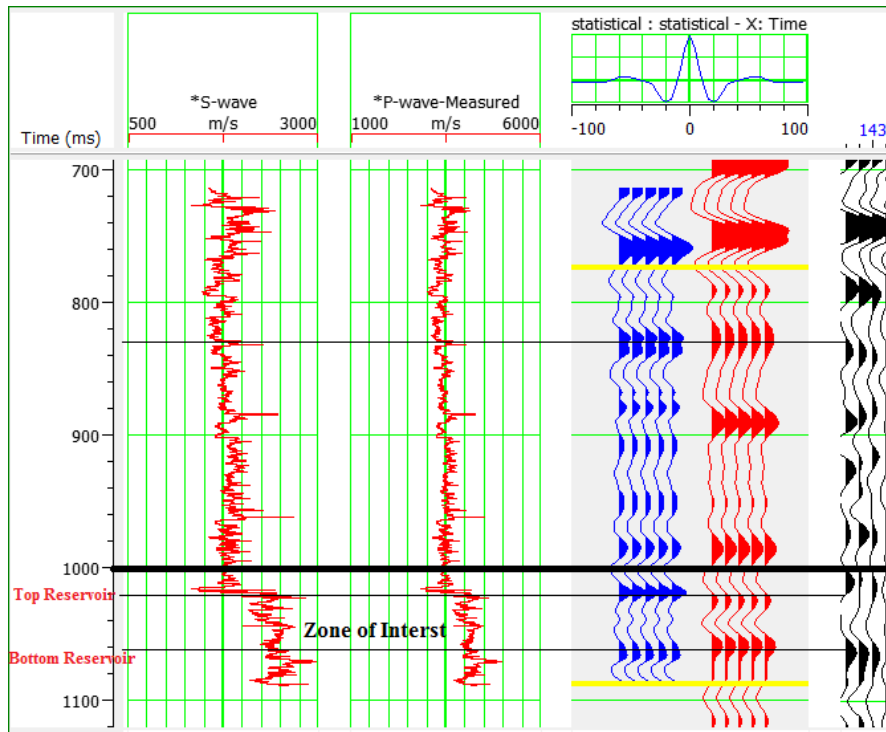


Fig. 6. Seismic well tie analysis for inversion process

4. Results and discussion

4.1. Wireline interpretation

Petrophysical properties (V_{sh} , SW and Porosity) were derived from the available wireline logs using conventional log analysis. However, this analysis was inadequate to achieve optimum separation of the upper and intra-Ordovician reservoir units and their unconformities. Especially the lower contact between Mamuniyat and Hawaz Formations, illustrated by red circle (Figure 7), even though a combination of porosity, gamma ray, sonic, neutron porosity and density was used with a particular colour template that reflects the cut-off values of shale and sand unit observed from all the wells. Furthermore, the gradual facies

change from the sandy-shale of Bir Tlaksin Formation to shaly-sand of the Upper Mamuniyat is not detected in the areas where the Bir Tlaksin Formation is thinner (Figure 7). The fluid substituted P-impedance shows a fit of the brine case (blue Curve) with original case (black Curve) confirming the fact of being a dry reservoir (Figure 8). Whereas the oil and gas cases showed lower PI values in sand zone and superimposed with the initial case at shale zones as expected (Figure 9).

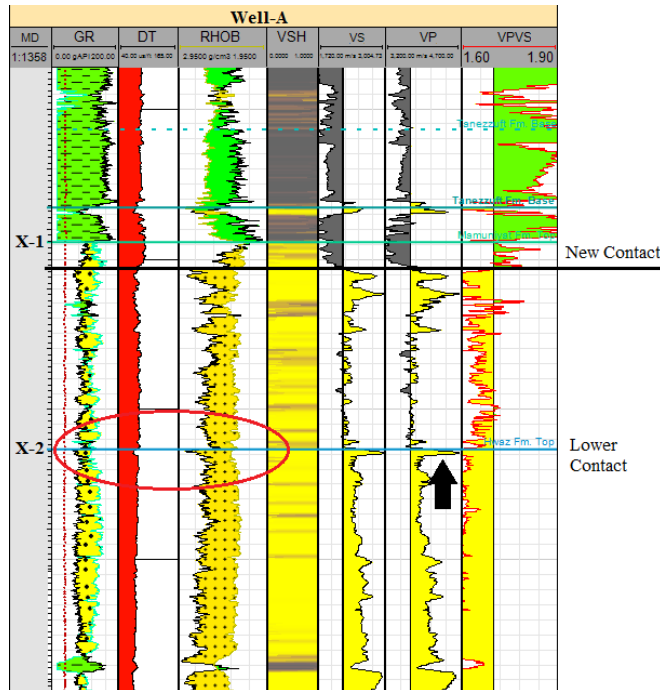


Fig. 7. Interpreted petrophysical properties (GR, Porosity, DT, RHOB and VSH) with elastic properties (Vp, Vs and VpVs) in Well A, showing the application of elastic properties sand and shale baselines and their effectiveness on picking Upper and Intra-Ordovician unconformities

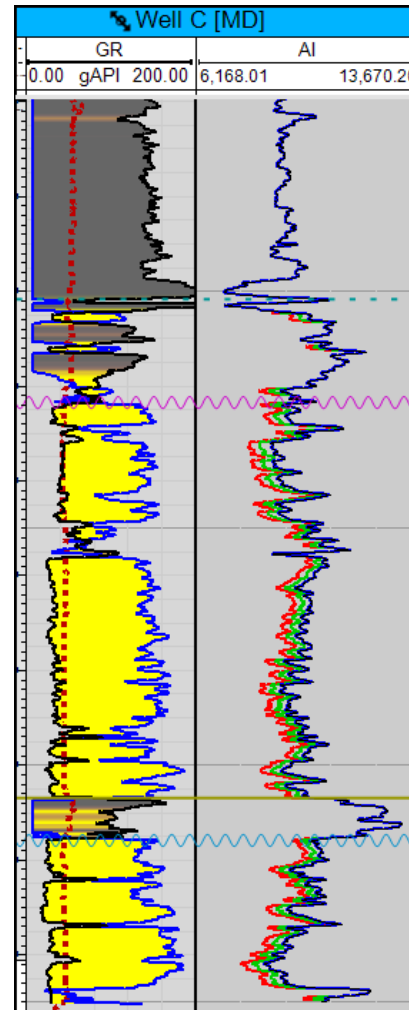


Fig. 8. Represents the result of the fluid substitution for three cases oil (green), gas (red), brine (blue) and original (black). The last is masked by brine curve confirming the original condition of this reservoir →→

4.1.1. Sand-shale elastic properties baseline cut-offs

Vs estimated using Greenberg-Castagna showed a closer fit to the measured shear wave in well A. Therefore, it was selected and used for velocity ratio calculation and input for petrol-elastic correlations. Vp, Vs and Vp/Vs ratio values for sand and shale units were identified by running several petro-elastic cross plots such as GR in the x-axis against GR/Vs (y-axis) (Figure. 10). The average values representing the lithology end members were then selected. Moreover, used as a baseline and colour the template on the correlation panel (Figure. 7). The elastic properties identified the top of the Upper Ordovician unconformity unit of Mamuniyat Formation and allowed shifting it a couple of meters down. Also, the intra-Ordovician unconformity on the top of Hawaz formation is delineated with an increase of both S and P waves

leading to a decrease of their ratio, which was due to abrupt change from the eroded lower dirty upper Ordovician reservoir to the top of the paleo-high Hawaz formation (Figure. 7).

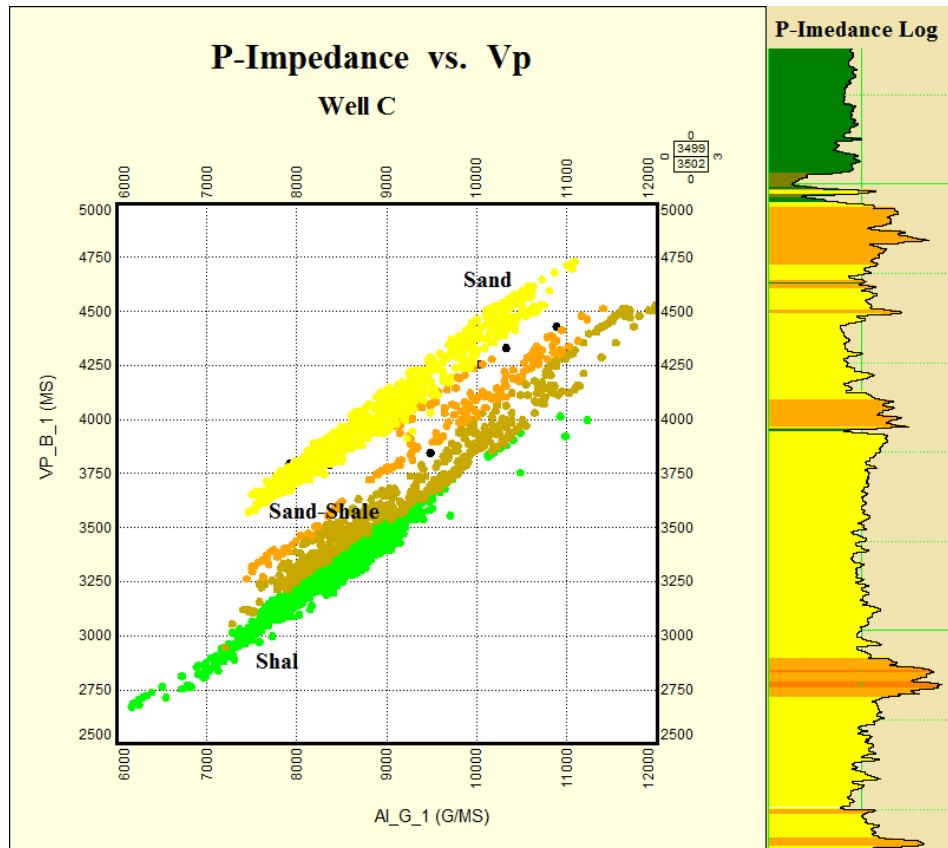


Fig. 9. The cross plot of P-Impedance gas case vs. Vp initial case showing the enhanced separation between sand shale facies after the fluid substitution application

4.1.2. Vp and Vs cross-over

The technique of 'log Cross-over' is widely used in wireline interpretation, especially neutron density logs, but it has not been implemented with elastic properties. This technique was adapted here using standard Vp scale and reverse Vs scale curves (Figure. 11). Sand cycles appear when the Vp (shown in red) is located on the right side of the track, whereas the appearance of Vp on the left side indicates the presence of shale units (Figure 11). The larger the separation between both curves (Vp and Vs), the cleaner the identified lithology. Conversely, the tighter the cross-over, the higher the mixture of sand and shale units. By applying this method, we were able to quickly identify the two main Ordovician unconformities and their internal zones. The upper Ordovician unconformity illuminated by sizeable thin separation followed by series of tight and larger separations with Vp curve to the right (Figure 12). While the second dirty zone of the upper Ordovician reservoir named M1 (Figure. 11), is characterised by a combination of tight and medium separations with Vp curve. The location of the Vp curve (right to the left) reflects the percentage of shale and sand for each layer. The lower zone top (M2) of the reservoir can be openly discriminated by a more consistent medium to small separation without an overlay of both curves and with a remarkable location of Vp to the left and Vs to the right within the whole zone. Finally, the lower contact of the reservoir can be identified either by; if the lower shaly member of Melaz Shuqran formation exists the contact delineated small separation with Vp curve to the left and Vs to the right such as in well C (figure. 11). However, if the above-stated formation is eroded the contact will be reflected by a significant funnel to bell separation with Vp curve to the right. The

distance of the crossover is controlled by the percentage and thickness of clean coarse sandstones of the top Hawaz unconformity (well B and A figure. 11).

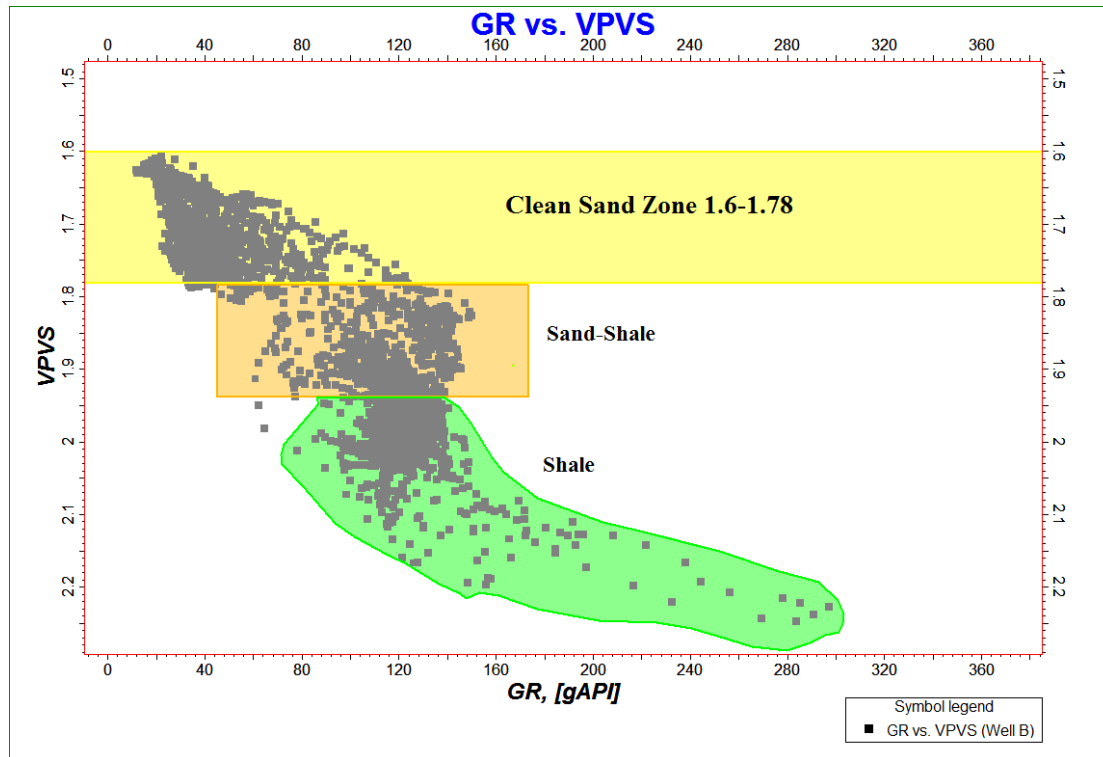


Fig. 10. The cross plot of Gamma ray log vs VpVs log, showing how the shale and sand cut-offs values were selected to be used for elastic properties estimation

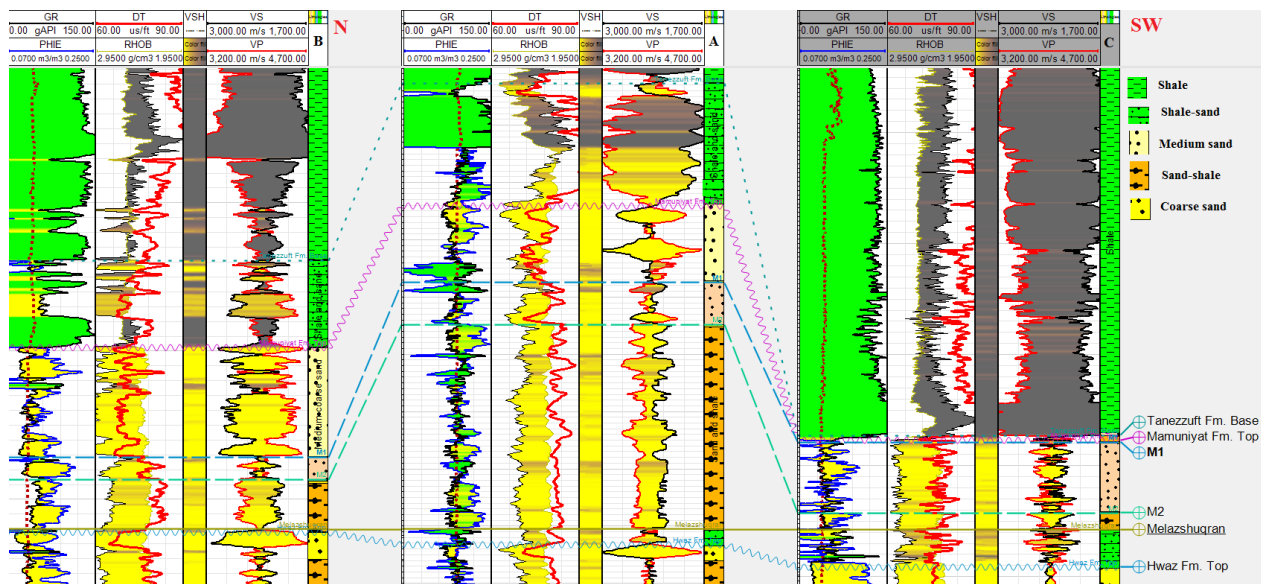


Fig. 11. N-SW Petro-elastic correlation panel for the tree wells representing the new suggested contacts of upper and Intra-Ordovician unconformities by the VP and Vs cross over nature

4.2. Conventional seismic interpretation

Structure maps of the Basement, Base Tanezzuft and Top Tigouentourine were generated from the interpreted 2D seismic lines. The Base Tanezzuft structure map showed the highest

relief in North, West and the central part of the study area, and the lowest relief in the south and south-east parts (Figure. 12). The identified structures may fall into two main trap types: Paleogeomorphologic traps that were generated as a result of glacial erosion during the Ordovician time when the melting glaciers cut through the Hawaz formation producing the erosion of its upper part. The Hawaz Formation then overlain by either the younger Silurian Tanezuft formation or in some areas of older Upper Ordovician Mamuniyat Formation. This trap type forms the most crucial plays in the Murzuq Basin, where the vast amounts of hydrocarbon were trapped within this basin. Inverted anticline Traps or Fault Blocks Traps which have been formed as a result of Cenozoic inversion: is mainly a structural three-way dip closures with an assumed sealed fault closing the fourth side in the Mamuniyat Formation and shares the same Hot Shale as the source rock with Tanezzuft shales as the seal. Thickness maps were generated to infer formation thicknesses covering between Base Tanezzuft and Basement shows that areas below the paleo-geomorphologic and inverted anticlines are thicker than the surrounding areas (Figure. 13).

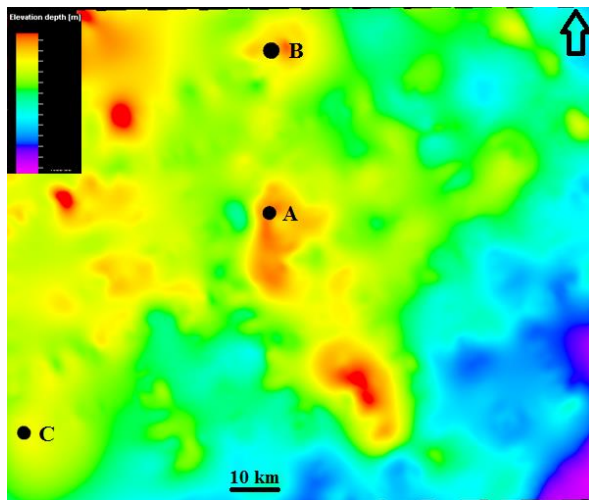


Fig. 12. Depth structure map of base Silurian 'Hot shale' interpreted using conventional 2D seismic data

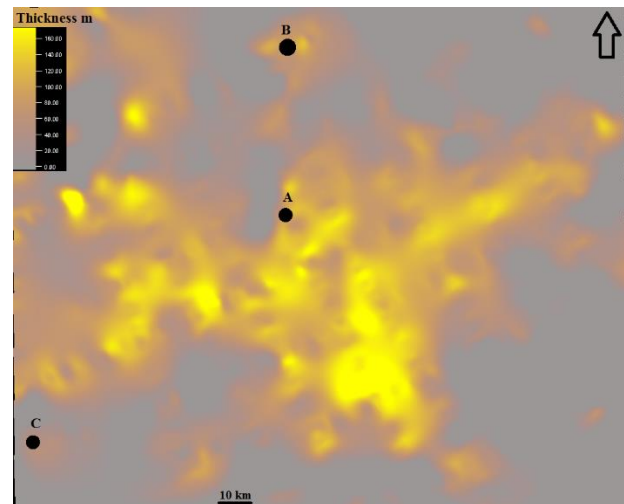


Fig. 13. Thickness map between Base Hot shale and basement. Representing the distribution of sand bodies in (yellow) and thinner in (dark grey)

4.3. Post Stack Seismic Inversion

A post-stack seismic inversion is a tool for inverting seismic trace into acoustic impedance to achieve practical geological results [21]. Post-stack inversion is a proper natural step to improve the stratigraphic interpretation units captured by post-stack seismic data. This type of seismic inversion has been universally used as an effective method for oil and gas exploration and production in several sedimentary basins. Usually, the primary focus of seismic inversion is to overcome the main challenges that might be encountered during the conventional seismic interpretation such as play system accurate delineation in the exploration level and estimation of petrophysical properties at the reservoir scale. Das *et al.* and Kumar *et al.* [22-23] stated the subsurface geology could be represented by stacked planes with parallel layers in all seismic inversion methods

The considered window for elastic properties estimation covers between 800-1175 ms. all values above or below this range might be erroneous.

In seismic Line X, the inverted impedance increases downward, except some upper and lower seismic sections that are not within the available well data. The significant change in acoustic impedance around 1025ms to 1075 ms of Well C indicates the top of Upper Ordovician reservoir, which overlies the short low impedance zone at 1100-1150ms indicating the Intra-Ordovician reservoir unit (Figure 14). In comparison to the original seismic line (Figure. 4), this inversion provided a better lateral and vertical events separation, which has improved the

traceability of the top reservoir event when compared to the original seismic data. The lower impedances are encountered at more shaly successions, while the medium impedances represent the sandy layers (Figure, 14). The section also represents a possibility of defining intra-Ordovician unconformity between the upper Ordovician Mamuniyat reservoir and Hawaz formation (Figures. 14).

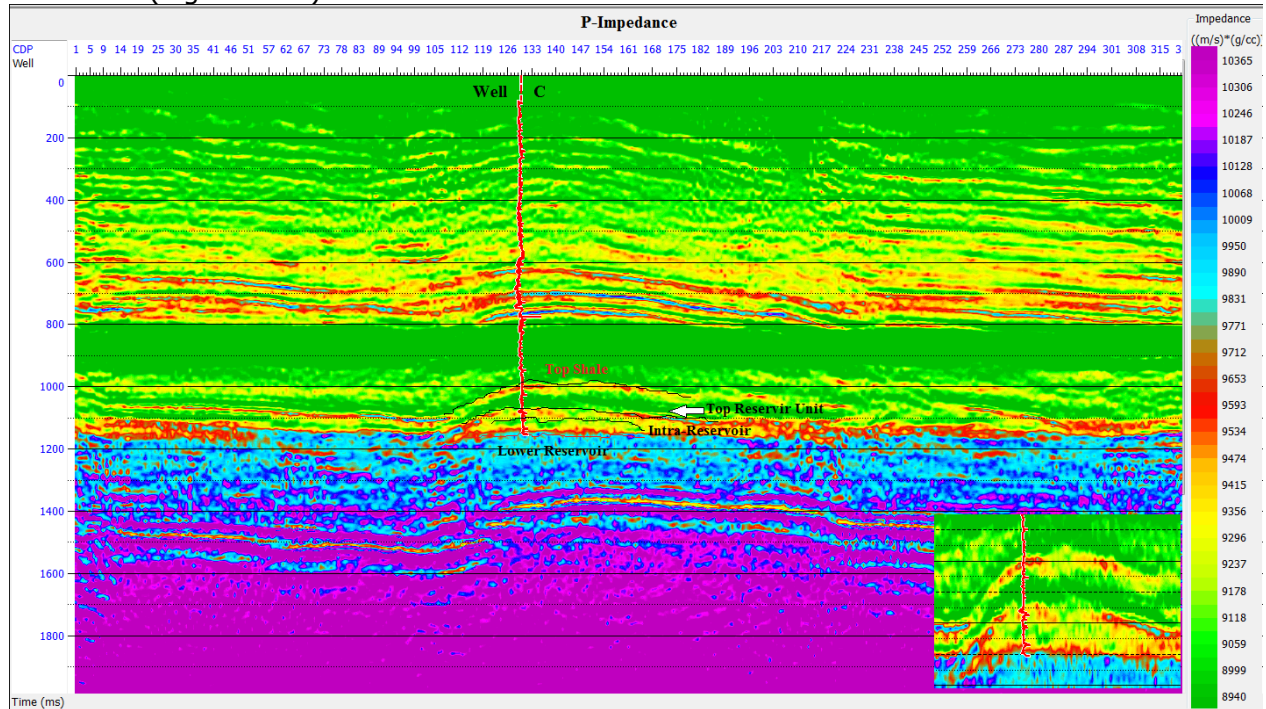


Fig. 14. Representing inverted acoustic impedance from seismic line X, with enhanced delineation of the upper Ordovician reservoir components

Using the above AI attributes, the primary structure has been delineated with a possibility of identifying the reservoir contacts and generate more accurate structure maps for the zones of interest (Figure. 14). The first top contact represents the shale zones and the second denotes the primary zone of interest (Top upper Ordovician reservoir) shown in Figure 14. The last two lines within the same figure suggest the intra-Ordovician reservoir unit and top Hawaz formation respectively.

Before modelling V_p/V_s from seismic, we cross-plotted Acoustic Impedance from seismic with V_p/V_s estimated from wells (Figure. 15) which has helped on classifying the lithological contents based on their elastic responses. The cross plot has enabled identification of four main lithological classes; 1) hot shale, with V_p/V_s of around 2.18 and PI of 5500-7700 (m/s)*(g/cc). 2) Shale contents with broader ranges of V_p/V_s (1.8-2) and PI (7700-9200 (m/s)*(g/cc)). 3) The sand zone which characterised by the range of 1.65-1.78 velocity ratio and 8700-10500 (m/s)*(g/cc) P-impedance. Finally, the mixed zone of shale-sand covers some parts of shale and sand zones (Figure. 15).

The predicted V_p/V_s from the seismic data (figure. 16) using neural network showed a better match to the one estimated from wells comparing to the curve generated using multi-attribute one (Figure. 16). Therefore, the former was used for generating V_p/V_s attribute from both 2D seismic lines.

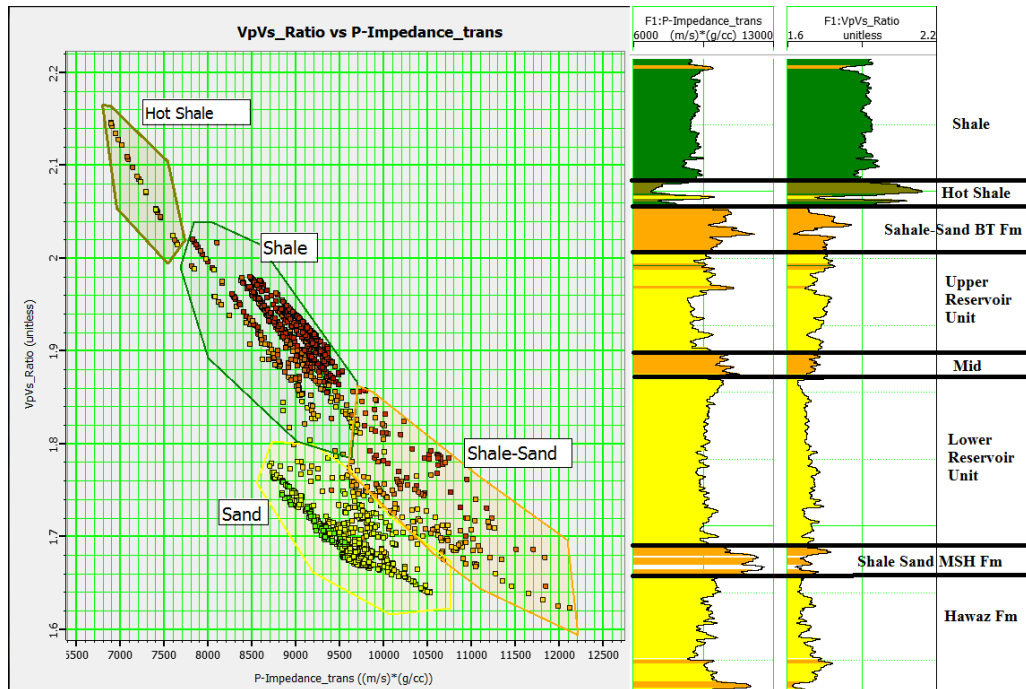


Fig. 15. The cross plot of P-Impedance vs. VpVs estimated from wells, which has helped on classifying the lithological contents based on their elastic responses. Namely, Hot shale (olive green), sand (yellow), Shale (Green) and shale Sand (orange)

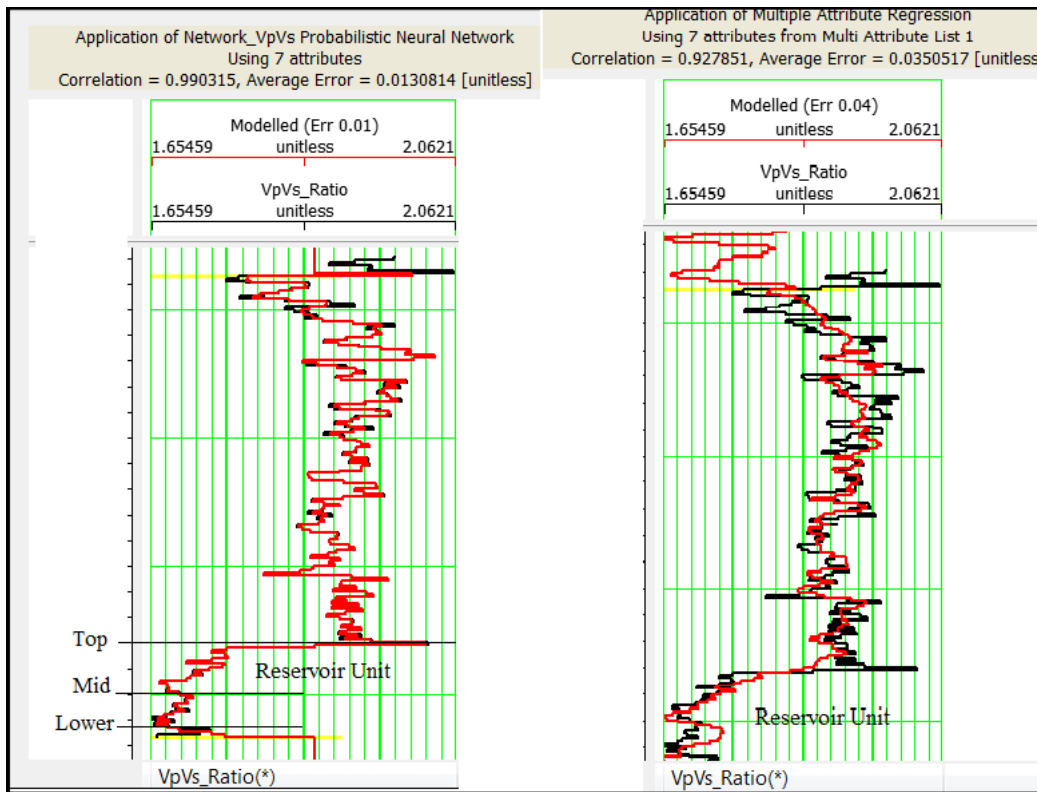


Fig. 16. Representing the comparison of predicted VpVs using probabilistic neural network (left) and multiple attribute regression using 7 attributes (right)

In the seismic section X, VpVs (Figure. 17) accurately predicted the top source rock formation at 1000ms near the well location, which continues in the opposite direction. Furthermore, the contact between Silurian Source rock and upper Ordovician reservoirs was precisely picked at 1100 ms near the well location. Unlike Acoustic impedance attributes, VpVs ratio picked the sand body as one set for this seismic section (Figure.17).

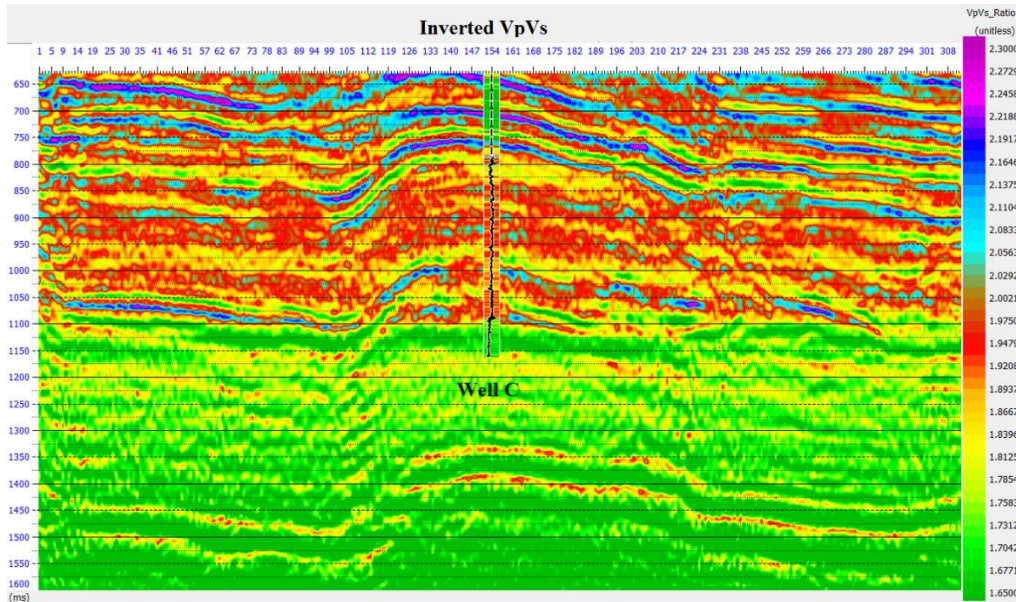


Fig. 17. Representing inverted Vp and Vs ratio at seismic line X, with precise delineation of the top reservoir at 1100 ms

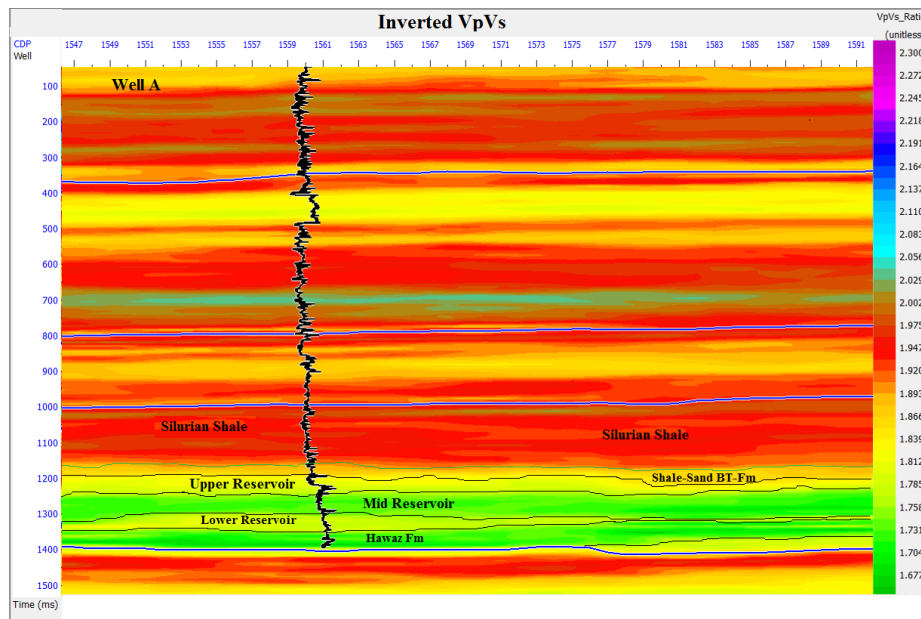


Fig. 18. Representing inverted Vp and Vs ratio from seismic line Y, showing the three main reservoir zones vertical and lateral distribution

For the seismic Line Y (Figure. 5), VpVs was generated using a workflow explained in the section 3.3.1. The VpVs attribute showed the reservoir area falls within the low percentage ratios between 1.6 and 1.8, which is the expected range for sand bodies with emphasis to their upper, mid and lower contacts (Figure. 18). Also showed how the interpreted horizons

using conventional seismic data did not manage to pick even some of the 'marker events' such as Horizons in Figure 18. Therefore, reinterpretation results can be reproduced by using the above-illustrated workflow, which indeed uncovers more facts on the lateral and vertical distribution of the primary producing reservoir by only utilising the existent database for this region.

5. Conclusion

This paper showed the effectiveness of combining petro-elastic correlation on enhancing the delineation of the upper Ordovician reservoir. The combination allowed the allocation of contacts between gradually interbedded clastic sediments. Also, the incorporation of simple elastic seismic attributes into prospect evaluation yielded a better delineation of the upper Ordovician main reservoir. By separating the sandy-shale of Bir Tlacsin formation from the upper reservoir unit in both seismic and wells, will undoubtedly improve the structural mapping of reservoir units by avoiding the assumption of using lower hot-shale contact as a top reservoir. It also provided vital details regarding the lithological variations and quality of the play fairways system in the South-South/West Murzuq Basin. Therefore, applying this simple, fast approach will help unearth specific features of petroleum systems by only reinterpreting the existing data set, which will hopefully trigger the exploration spotlight to this area again.

Acknowledgments

We would like to send our special gratitude to NOC for their cooperation and giving the permission to publish this paper. Our thanks also goes to Dr Adnan Aqrabi for his constructive comments and advice.

References

- [1] Craig J, Rizzi C, Said F, Thusu B, Luning S, Asbali A, Keeley M, Bell J, Durham M, Eales M. Structural styles and prospectivity in the Precambrian and Palaeozoic hydrocarbon systems of North Africa. *The Geology of East Libya*, 2008; 4: 51-122.
- [2] Craig J, Grigo D, Rebora A, Serafini G, Tebaldi E. From Neoproterozoic to Early Cenozoic: exploring the potential of older and deeper hydrocarbon plays across North Africa and the Middle East. Geological Society, London, Petroleum Geology Conference series 2010. Geological Society of London, pp. 673-705.
- [3] Davidson L, Beswetherick S, Craig J, Eales M, Fisher A, Himmali A, Jho J, Mejrab B, Smart J. The structure, stratigraphy and petroleum geology of the Murzuq Basin. *Southwest Libya-Chapter 2009*:14.
- [4] Davidson L, Beswetherick S, Craig J, Eales M, Fisher A, Himmali A, Jho J, Mejrab B, Smar, J. The structure, stratigraphy and petroleum geology of the Murzuq Basin, Southwest Libya. *Geological Exploration of the Murzuq Basin*. Elsevier, Amsterdam 2000: 295-320.
- [5] El Diasty WS, El Beialy S, Anwari T, Batten D, 2017. Hydrocarbon source potential of the Tanezzuft Formation, Murzuq Basin, south-west Libya: An organic geochemical approach. *Journal of African Earth Sciences*, 2017; 130: 102-109.
- [6] Galushkin Y, Eloghbi S, Sak M. 2014. Burial and thermal history modelling of the Murzuq and Ghadames Basins (Libya) using the GALO computer programme. *Journal of Petroleum Geology*, 2014; 37: 71-93.
- [7] Hallett D, Clark-Lowes D. *Petroleum geology of Libya*. Elsevier 2017.
- [8] Ron Martin MR, Erquiaga M, Blake B, Buitrago J, Reveron J, Obregon F, Cobos C, González Muñoz JM. Seismic Expression of Intra-Ordovician Unconformities in Murzuq Basin (Libya) through Pre-stack Inversion & Modelling, 2016.
- [9] Abushalah Y, Serpa L. Using instantaneous frequency and coloured inversion attributes to distinguish and determine the sandstones facies of the Late Ordovician Mamuniyat reservoir, R-field in Murzuq Basin. *Libya. Interpretation 4*, T507-T519, 2016.
- [10] El-Ghali MAK. Depositional environments and sequence stratigraphy of paralic glacial, paraglacial and postglacial Upper Ordovician siliciclastic deposits in the Murzuq Basin, SW Libya. *Sedimentary Geology*, 2005; 177: 145-173.

- [11] Abouessa A., Diagenetic properties of the Hawaz Formation, Murzuq Basin, Libya, Fourth Symposium on the Sedimentary Basins of Libya. The Geology of Southern Libya, 2012: 47-82.
- [12] Aziz A. 2000. Stratigraphy and hydrocarbon potential of the Lower Palaeozoic succession of License NC-115, Murzuq Basin, SW Libya-Chapter 16.
- [13] Le Heron D, Meinhold G, Elgadry M, Abutarruma Y, Boote D. Early Palaeozoic evolution of Libya: perspectives from Jabal Eghei with implications for hydrocarbon exploration in Al Kufrah Basin. Basin Research, 2015; 27: 60-83.
- [14] Denis M, Guiraud M, Konaté M, Buoncristiani J-F. Subglacial deformation and water-pressure cycles as a key for understanding ice stream dynamics: evidence from the Late Ordovician succession of the Djado Basin (Niger). International Journal of Earth Sciences, 2010; 99: 1399-1425.
- [15] Dupouy M, Desaubliaux G, Nosjean N, Lloyd A, Cherif R. Integrated sedimentological case study of glacial Ordovician reservoirs in the Illizi Basin, Algeria, 79th EAGE Conference and Exhibition 2017-Workshops.
- [16] Girard F, Ghienne J.-F, Rubino J-L, Channelized sandstone bodies ('cordons') in the Tassili N'Ajjer (Algeria & Libya): snapshots of a Late Ordovician proglacial outwash plain. Geological Society, London, Special Publications, 2012; 368: 355-379.
- [17] Moreau J, Joubert J-B. Glacial sedimentology interpretation from borehole image log: Example from the Late Ordovician deposits, Murzuq Basin (Libya). Interpretation, 2016; 4: B1-B16.
- [18] Le Heron D, Armstrong H, Wilson C, Howard J, Gindre L. Glaciation and deglaciation of the Libyan Desert: the Late Ordovician record. Sedimentary Geology, 2010; 223: 100-125.
- [19] Shalbak FA. Palaeozoic petroleum systems of the Murzuq Basin. Libya 2015.
- [21] Das B, Chatterjee R, Singha DK, Kumar R. 2017. Post-stack seismic inversion and attribute analysis in shallow offshore of Krishna-Godavari basin, India. Journal of the Geological Society of India, 2017; 90: 32-40.
- [22] Kumar R, Das B, Chatterjee R, Sain K. 2016. A methodology of porosity estimation from inversion of post-stack seismic data. Journal of natural Gas science and engineering, 2016; 28: 356-364.
- [23] Lee K, Yoo D, McMechan GA, Hwang N, and Lee GH. A Two-Dimensional Post-Stack Seismic Inversion for Acoustic Impedance of Gas and Hydrate Bearing Deep-Water Sediments Within the Continental Slope of the Ulleung Basin, East Sea, Korea. Terrestrial, Atmospheric & Oceanic Sciences, 2013; 24(3): 295-310.
- [24] McDougall ND, Tawengi K, JG Quin, and Vila Pont J. Depositional environments and largescale sediment architecture in the Upper Ordovician of the Murzuq Basin, SW Libya (Melaz Shuqran and Mamuniyat Formations, EAGE, 2nd North African/Mediterranean Petroleum and Geoscience Conference 2005, Abstract volume, 8.

To whom correspondence should be addressed: Abubaker Alansari, Department of Geosciences, University Technology PETRONAS, 32610, Perak, Malaysia